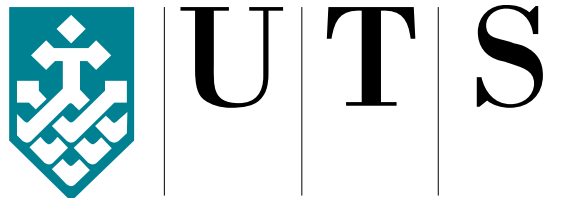


# **PATIENT SPECIFIC 3D FINITE ELEMENT MODELLING, ANALYSIS AND VERIFICATION OF DENTAL IMPLANT NAVIGATION AND INSERTION SYSTEM**



**Valerio Taraschi**

School of Mathematical and Physical Sciences

University of Technology - Sydney

This dissertation is submitted for the degree of

*Doctor of Philosophy*

August 2016



## **Declaration**

This thesis is the result of a research candidature conducted jointly with another University as part of a collaborative Doctoral degree. I certify that the work in this thesis has not previously been submitted for a degree nor has it been submitted as part of requirements for a degree except as part of the collaborative doctoral degree and/or fully acknowledged within the text.

I also certify that the thesis has been written by me. Any help that I have received in my research work and the preparation of the thesis itself has been acknowledged. In addition, I certify that all information sources and literature used are indicated in the thesis.

Valerio Taraschi

August 2016

## **Acknowledgements**

First and foremost I would like to express my gratitude to my supervisor Professor Besim Ben-Nissan, for sharing his immense and passionate knowledge with me during this research work, for guiding my professional growth in the last years and for his enlightening friendship.

I would also like to thank my co-supervisor Professor Bruce Milthorpe for directing this long research journey with wisdom regardless of his numerous commitments.

A special acknowledgement goes to BresMedical's General Management for their contribution to this research by allocating resources in assisting with the development of the navigation system. In particular, I would like to express my gratitude to the technical work of Daniele Giunchi, Waldemar Rostek, Soong Vongbunyong, Chris Dodson, Mel McNair and Mark Helou and to the significant support offered by Kevin Cullen, Tracy Rix and Marcos Perez.

For their remarkable clinical contribution in assisting with the design of the navigation system, for performing Clinical Trials and for making software packages available to this research I would also like to acknowledge Dr Gerardo Pellegrino and Professor Marchetti from University of Bologna.

I would like to thank my supporting and lovely wife Sarah for making my life better and more meaningful every day.

Last but not least, thanks to my always caring now asleep mother and father and my sisters who have always encouraged me from Italy.

## **Abstract**

The use of a biomechanically correct finite element model (FEM) for simulating the behaviour of the human mandible during functional movements can be improved by including patient-specific anatomical data and real bone density data derived from a tomographic scan.

A model produced through this approach could be more realistic than the ones reported in literature over the last decades which lack subject-specificity in terms of morphological features and local material properties. Most of the published models over-constrain the mandible and do not include the action of facial muscles leading to what this study proves being simplistic or even erroneous interpretations of crucial implant osseointegration processes.

By interpreting tomographic data, in this research work the author developed advanced FEMs of the human mandible applied to realistic clinical scenarios and which can therefore be used to guide treatment plans.

Finite element simulations were also created to validate the design and the mechanical stability of a dimensionally reduced implant-supported patient reference tool used with an innovative and minimally invasive image-guided surgery system.

The author developed such novel navigation system for oral implantology to allow surgical approaches which otherwise could be not pursued using traditional techniques. This task required the design and prototype of software and hardware components which are now being clinically tested.

This thesis shows the application of the navigation system to the insertion of long angled implants for posterior support of full-arch prostheses. From the results of the FEM and by taking into account the micro-motions of the inserts generated by the full set of muscular

forces acting on a mandible in mechanical equilibrium under functional loading, this configuration showed superior osseointegration potential as opposed to what is reported in literature.

The author also applied the FEM to evaluate the osseointegration potential of implants with deep cortical anchorage, as opposed to shorter mono-cortical implants.

Moreover, a novel procedure for their safe insertion was designed by combining the benefits of ultrasonic bone socketing (piezoelectric osteotomy) with the dynamic guidance offered by the developed navigation system.

In force of its clinical potential, the surgical approach proposed in this study is currently being validated through in vivo trials approved by the independent ethical committee of University of Bologna. Preliminary results from Clinical Trials, as presented in this work, reported an average accuracy for implant insertion of  $0.90\pm 0.07$  mm.

It is reasonable to state that the ultimate conclusion of this investigation is that the developed image-guided surgery system can be used safely and for significant outcomes on a routine basis for orthodontic or maxillofacial surgical procedures.

On the other hand the simulation designed to investigate its safe use on a patient is potentially suitable to determine the impact of patient-specific treatment procedures for ideal prosthetic restorations and to simulate the behaviour of other implantable components.

# Table of contents

<b>List of figures</b>	<b>xiv</b>
<b>List of tables</b>	<b>xxii</b>
<b>1 Introduction</b>	<b>1</b>
1.1 Mandibular model . . . . .	2
1.2 Biomechanical Approach and FEA . . . . .	2
1.3 FEM models and differentiation criteria: materials, constraints, data acquisition . . . . .	3
1.4 Proposed FEA model: assumptions . . . . .	7
1.4.1 Material mapping . . . . .	7
1.4.2 Biomechanics of the mandible . . . . .	7
1.4.3 The anatomy of the mandible . . . . .	8
1.4.4 Musculature . . . . .	8
1.4.5 Biomechanical equilibria and the reaction force . . . . .	9
1.4.6 Reaction force positioning issue . . . . .	11
1.4.7 Load application . . . . .	12
1.4.8 Finite element analysis application issues . . . . .	12
1.5 Anticipation of research products and outline of the thesis . . . . .	13
1.6 Future developments . . . . .	15
<b>2 Preparation of a patient-matched biomechanically correct Finite Element Model of the human mandible for the evaluations of clinical scenarios</b>	<b>16</b>

---

2.1	What is a Finite Element Model of the mandible . . . . .	16
2.2	Three-dimensional model design procedure . . . . .	17
2.2.1	Complexity of exterior shape and interior structure of the mandible	17
2.2.2	Influence of the morphological complexity on the modelling . . .	20
2.2.3	Bone surface reverse-engineering . . . . .	20
2.2.4	The importance of Meshing . . . . .	21
2.3	Pre-processing the finite element model . . . . .	23
2.3.1	The choice of material properties and analysis types . . . . .	24
2.3.2	Loading and boundary conditions . . . . .	26
2.3.3	Cortical bone variations . . . . .	27
2.3.4	Cancellous bone properties . . . . .	28
2.3.5	Interface between bone types . . . . .	32
2.3.6	Choice of material properties . . . . .	33
2.3.7	Biomechanical considerations . . . . .	33
2.3.8	Algorithm for assigning nodal forces . . . . .	34
2.4	Use of subject-specific material properties derived from CT scan data . .	35
2.4.1	Relation between HU and Density . . . . .	35
2.4.2	Mapping density and elasticity . . . . .	42
2.5	Applications of the FEA . . . . .	44
<b>3</b>	<b>FEM application to a new surgical navigation system reference frame</b>	<b>46</b>
3.1	Introduction . . . . .	46
3.2	Background . . . . .	47
3.3	Materials and Methods . . . . .	49
3.3.1	Image-guided Surgery System . . . . .	49
3.3.2	FEMs and scenarios . . . . .	51
3.3.2.1	M1a modelling . . . . .	52
3.3.2.2	M1b modelling . . . . .	55
3.3.2.3	M2 modelling: accidental interference . . . . .	56
3.3.2.4	M3 modelling . . . . .	63

---

3.4	Results and Discussion . . . . .	64
3.4.1	M1a model . . . . .	66
3.4.2	M1b model . . . . .	71
3.4.3	M2 model . . . . .	74
3.4.4	M3 model . . . . .	75
3.5	Clinical considerations and Conclusions . . . . .	88
<b>4</b>	<b>Effects of deep cortical and angulated implants-supported prostheses on the osseointegration process by a Finite Element Study</b>	<b>92</b>
4.1	Introduction . . . . .	92
4.2	Background . . . . .	93
4.2.1	Use of dental implants . . . . .	93
4.2.2	Insertion procedure . . . . .	94
4.2.3	Influence of peri-implant stresses on osseointegration . . . . .	95
4.2.4	Influence of implant diameter and loading direction on osseointegration . . . . .	96
4.2.5	Bone-implant interface . . . . .	99
4.2.6	The problem with larger implants . . . . .	100
4.2.7	Posterior mandible preparation . . . . .	100
4.2.8	Double-cortical ultrasonic preparation . . . . .	104
4.2.9	Biomechanics of the mandible . . . . .	106
4.2.10	Factors influencing the insertion of an implant and summary of hypotheses . . . . .	107
4.2.11	Biomechanical and clinically relevant output of the present model	109
4.3	Method . . . . .	109
4.3.1	Implant Planning . . . . .	109
4.3.2	Biomechanical models . . . . .	111
4.3.3	FEM pre-processing . . . . .	112
4.3.4	Control groups . . . . .	113
4.3.5	Significance of control group I4c1 . . . . .	115

---

4.3.6	Implant position planning for I1 and I1c . . . . .	118
4.3.7	Load set and boundary conditions . . . . .	122
4.3.8	Comparison with fully constrained model . . . . .	125
4.3.9	Material properties and pre-processing . . . . .	125
4.3.10	Post-processing . . . . .	126
4.4	Results . . . . .	127
4.4.1	Angled insertion versus axial implants . . . . .	127
4.4.2	Deep cortical anchorage versus larger implants . . . . .	133
4.5	Discussion . . . . .	137
4.5.1	All-on-Four <sup>®</sup> and osseointegration . . . . .	137
4.5.2	Deep cortical implant planning . . . . .	139
4.6	Conclusions . . . . .	140
<b>5</b>	<b>A critical review of currently used Image Guided and Computer-Assisted Surgery systems: current research, state-of-the-art models, techniques used for image-to-world registration and analysis of invasiveness</b>	<b>142</b>
5.1	Introduction . . . . .	142
5.2	Computer-assisted surgery and the use of drill guides . . . . .	143
5.3	Problems associated with the use of drill guides . . . . .	150
5.3.1	Limited access and visibility . . . . .	150
5.3.2	Invasiveness . . . . .	151
5.3.3	Delay . . . . .	151
5.3.4	Accuracy . . . . .	152
5.4	Image-guided surgery as alternative to CAS drill guides . . . . .	153
5.4.1	Stryker: II-Cart (3D C-ARM Registration vs Pair Point) . . . . .	155
5.4.2	Medtronic: O-ARM and Stealth TREON . . . . .	155
5.4.3	Claron: Navident <sup>®</sup> . . . . .	157
5.4.4	BBraun: OrthoPilot . . . . .	158
5.4.5	Blue Belt Technologies: Navio PFS . . . . .	158
5.4.6	BrainLab: Vector Vision . . . . .	160

---

5.4.7	x-Nav . . . . .	164
5.5	Discussion . . . . .	166
5.5.1	Invasiveness . . . . .	166
5.5.2	Visibility . . . . .	167
5.5.3	Dynamic approach in surgery . . . . .	167
5.5.4	Clinical relevance . . . . .	168
5.6	Concluding Remarks on CAS systems . . . . .	170
<b>6</b>	<b>Design, development and analysis of a new and unique Navigation System for oral image-guided implantology, focus on an innovative miniaturized reference tool, dedicated software application, registration procedure, hardware-software integration</b>	<b>172</b>
6.1	Introduction . . . . .	172
6.2	Method of development and procedure . . . . .	174
6.2.1	General hardware requirements . . . . .	174
6.2.2	General software requirements . . . . .	175
6.3	Design . . . . .	175
6.3.1	System components . . . . .	175
6.3.2	Operational workflow . . . . .	176
6.3.3	Surgical drill guide template workflow . . . . .	177
6.3.4	Image guided surgery navigation workflow . . . . .	179
6.3.5	Registration procedure: software design . . . . .	183
6.3.6	Registration procedure: hardware components . . . . .	185
6.3.7	Centroids experiment . . . . .	186
6.3.8	Patient registration: edentulous or partially edentulous case . . . . .	189
6.3.9	Calibration procedure: hardware design . . . . .	190
6.3.10	Additional hardware design for live tracking . . . . .	192
6.3.10.1	Optical reference supports . . . . .	192
6.3.10.2	Double-joint . . . . .	193
6.3.10.3	Handpiece attachments . . . . .	196

---

6.3.11	GUI Design . . . . .	197
6.3.11.1	GUI: surgical planning . . . . .	197
6.3.11.2	GUI: surgical navigation . . . . .	199
6.4	Analysis and verification . . . . .	201
6.5	Conclusions . . . . .	202
<b>7</b>	<b>Pre-Clinical trials: application of a new intra-oral navigation system to piezo- electric surgery for three-dimensional implant site preparation</b>	<b>205</b>
7.1	Introduction . . . . .	205
7.2	Piezoelectric surgery for oral implantology . . . . .	207
7.3	Materials and Methods . . . . .	208
7.3.1	Surgical plan . . . . .	208
7.3.2	Calibration . . . . .	210
7.3.3	Patient-scan registration . . . . .	213
7.3.4	Surgical technique and cases . . . . .	214
7.3.5	Accuracy evaluation . . . . .	218
7.3.6	Post-operative corrections . . . . .	219
7.4	Results and Discussion . . . . .	219
7.5	Conclusions . . . . .	223
<b>8</b>	<b>Major contributions of the thesis to science and knowledge</b>	<b>224</b>
	<b>Glossary</b>	<b>227</b>
	<b>Appendix Appendix A</b>	<b>231</b>
	<b>Appendix Appendix B</b>	<b>259</b>
	<b>References</b>	<b>264</b>

# List of figures

1.1	Musculature loads set . . . . .	9
1.2	Condyle reaction force application . . . . .	12
2.1	Morphologically different bone samples . . . . .	18
2.2	Example of modelling the bone-implant interface . . . . .	24
2.3	Stress profiles along bone-implant interface . . . . .	30
2.4	Example of segmentation using a “threshold” function . . . . .	31
2.5	Examples of cortical-cancellous bone model approximation . . . . .	32
2.6	Sampling CT numbers in the scan . . . . .	36
2.7	Representation of the mesh in Bonemat . . . . .	44
3.1	Reference frame assembly for navigation . . . . .	51
3.2	Visual representation of muscle force vectors. . . . .	59
3.3	Section of a mandible model with an implant-supported reference tool. . . . .	60
3.4	Different implants used in M2 modelling . . . . .	62
3.5	Example simulation results for deformation . . . . .	66
3.6	Deformation during clenching . . . . .	67
3.7	Deformation during wide opening . . . . .	68
3.8	Stress distribution during clenching . . . . .	69
3.9	Regions of equivalent stress higher than 75 MPa during clenching . . . . .	69
3.10	Probing of the equivalent stress in the molar region . . . . .	70
3.11	von Mises stresses in the mandible (Choi 2005) . . . . .	70
3.12	Equivalent stress along longitudinal path on implant surface . . . . .	72

---

3.13	Stress distribution on the implant during scan . . . . .	73
3.14	Anteroposterior view of the mandible under stress during surgery . . . . .	74
3.15	Stress distribution due to accidental vertical hit down during scan . . . . .	75
3.16	Stress distribution due to accidental vertical hit in cancellous bone. . . . .	76
3.17	Stress distribution on the MINI-implant during an accidental vertical hit . . . . .	76
3.18	Distribution of CT numbers in the mandibular mesh . . . . .	77
3.19	Frequency of Young's Moduli in the mandible mesh . . . . .	79
3.20	Relation between CT numbers and density . . . . .	80
3.21	Bonemat GUI . . . . .	81
3.22	Colour bands corresponding to deformation during clenching . . . . .	83
3.23	Results for deformation during clenching visualised in Ansys Workbench Mechanical. . . . .	83
3.24	Equivalent stresses in the molar regions during clenching . . . . .	84
3.25	Equivalent stresses during clenching showing high stresses on the coronoid processes . . . . .	84
3.26	Deformed shape versus undeformed shape during wide opening movement	85
3.27	Mandibular distortion during wide opening movement . . . . .	85
3.28	Colour bands corresponding to deformation during wide opening . . . . .	86
3.29	Equivalent stresses during wide opening showing higher stresses on the coronoid processes . . . . .	86
3.30	Frequency of calculated densities in the mandible mesh . . . . .	87
3.31	Distribution of Young's moduli in the finite element mesh calculated using an inverse approach . . . . .	87
4.1	Graphic representation of vertical and buccolingual load . . . . .	98
4.2	Increased antero-posterior spread achieved by the use of tilted implants . . . . .	102
4.3	Posterior unsupported extension of an overdenture . . . . .	103
4.4	Rotary drill tip's misalignment with the prosthetic axis due to an implant shift . . . . .	105
4.5	Software view which allows the creation of a panoramic profile . . . . .	110

4.6	Compound view of the scanned anatomy during the implant virtual planning operation . . . . .	111
4.7	Superposition of the I4 and I4c2 scenarios in the virtual planning environment	113
4.8	Virtual planning for the control group I4c1 . . . . .	114
4.9	Typical assembly for single tooth prostheses . . . . .	114
4.10	CAD modelling of the overdenture used in the finite element simulations .	115
4.11	Three-dimensional model of the human mandible used in the presented FEMs . . . . .	116
4.12	Virtual planning relative to the scenario I4c2 . . . . .	118
4.13	Measurement of the distance between a posterior axial implant and the adjacent dental nerve . . . . .	119
4.14	“Steps” used for bite force on an implant-supported prosthesis . . . . .	119
4.15	Deep cortical anchorage versus crestal-only cortical preparation . . . . .	120
4.16	Piezosurgery <sup>®</sup> inserts for ultrasonic differential preparation of the implant socket . . . . .	121
4.17	activation of the muscles involved in the biting action . . . . .	122
4.18	Probing of stresses along the implant socket . . . . .	126
4.19	Probing line orientation by deformation pattern . . . . .	127
4.20	Von Mises stress distribution on the mandible relative to model I4 . . . . .	128
4.21	Equivalent stress distribution relative to I4 . . . . .	128
4.22	Equivalent stress distribution on the posterior right implant surface relative to I4 and I4c1 . . . . .	130
4.23	Equivalent stress distributions and maximum values obtained for a left posterior angled implant in I4 and I4c1 . . . . .	130
4.24	Equivalent stress curves for the left and right posterior implants by longitudinal probing . . . . .	134
4.25	Equivalent stress curves for the left posterior implants by radial probing .	135
4.26	Deep cortical anchorage used in model I1 . . . . .	136
5.1	Digitisation of a prosthetic component using NobelProcera laser scanner .	144

---

5.2	CBCT data viewing and surgery planning using NobelClinician™ . . . . .	145
5.3	Examples of dental drill guides for partially edentulous patients . . . . .	145
5.4	Radiopaque markers in the radiographic template . . . . .	146
5.5	Surgical guide for edentulous cases . . . . .	146
5.6	Materialise edentulous surgical guide design in bone-supported case . . . . .	147
5.7	Materialise edentulous surgical guide design in mucosa-supported case . . . . .	147
5.8	Materialise teeth-supported surgical guide design . . . . .	148
5.9	Materialise surgical drill guide application . . . . .	148
5.10	Sirona virtual surgery planning . . . . .	148
5.11	Sirona surgical guide design . . . . .	149
5.12	Sirona surgical guide placement during surgery . . . . .	149
5.13	All-on-4® treatment concept for full mandibular arch restoration . . . . .	150
5.14	Stryker navigation system assembly . . . . .	156
5.15	Strong's experimental setup . . . . .	157
5.16	Navident navigation system . . . . .	159
5.17	Digitization of patient's knee and OrthoPilot's software interface . . . . .	160
5.18	Blue Belt's Navio PFS probe . . . . .	160
5.19	Snapshot of Brainlab's navigation software application . . . . .	162
5.20	Model showing splint used for registration . . . . .	163
5.21	Titanium screws used as fiducial markers . . . . .	163
5.22	Occlusal splint with five hexagonal-headed screws . . . . .	164
5.23	Self-drilling screws fixed on the superior orbital frame . . . . .	165
5.24	ClaroNav's handpiece reference frame and patient's gig . . . . .	168
6.1	Schematic representation of the main components of a surgical navigation system . . . . .	176
6.2	Digital extraction of fiducial markers . . . . .	178
6.3	Drilling sequence with preparation via surgical guide without the insertion of a drill extender . . . . .	180
6.4	Drilling sequence with preparation via surgical guide using drill extenders . . . . .	181

---

6.5	CAD model and physical prototype for piezoelectric handpiece long probe calibration . . . . .	184
6.6	Picking of radiopaque markers with a piezoelectric handpiece calibration probe . . . . .	184
6.7	Fiducial radiopaque markers . . . . .	186
6.8	Visualisation of the isosurfaces of the radiopaque markers at different threshold values . . . . .	187
6.9	Design of a Titanium screw used as fiducial marker . . . . .	188
6.10	Fiducial markers plate for edentulous patients . . . . .	189
6.11	Fiducial markers tray for partially edentulous patients . . . . .	190
6.12	Original design for a calibrating instrument . . . . .	191
6.13	Movement required for drill tip calibration . . . . .	192
6.14	CAD model of the developed reference tool assembly . . . . .	194
6.15	“Double-joint” connecting the fiducial markers holder and the optical reference frame . . . . .	194
6.16	Reference assembly facing the tracking camera in two operational positions	195
6.17	Reference assembly applied to two different surgical techniques . . . . .	196
6.18	Virtual planning stage in the developed software application . . . . .	198
6.19	Virtual prosthesis visualisation during implant planning . . . . .	199
6.20	Navigation operation views . . . . .	200
6.21	Concept setup of the developed surgical navigation system . . . . .	202
6.22	Display device used to output the information of the navigation system . . . . .	203
6.23	Use of reference tool system on a Piezosurgery® handpiece . . . . .	204
7.1	Piezosurgery® kit for dental implantology and relative sequence of utilisation	209
7.2	Socket preparation and implant insertion using Piezosurgery® differential preparation . . . . .	209
7.3	Surgical plan using the developed compound view of the software application	210
7.4	Virtual tooth function . . . . .	211
7.5	Curved tip calibration device . . . . .	212

---

7.6	Reference frame supporting the plastic reflective balls . . . . .	213
7.7	Reference plates for partially and totally edentulous patients . . . . .	214
7.8	Implant shift due to the contact between the tip and the lingual cortical wall	215
7.9	Software interface showing the selective preparation of the lingual cortical wall using the IMS1 and IM2P inserts . . . . .	216
7.10	Steps of a full piezo-navigated implant site preparation using only two Piezosurgery® inserts . . . . .	216
7.11	Position of the Piezosurgery® tip while tracked live on the patient . . . . .	217
7.12	Live tracking of implant insertion . . . . .	217
7.13	Alignment of the pre-operative scan and the post-operative volume . . . . .	218
7.14	Superposition of post-operative implant with planned implant . . . . .	220
1	Model I4: deformation of anterior left and right implants in complete muscle load set biomechanical configuration . . . . .	232
2	Model I4: micro-motions of posterior left and right implants in complete muscle load set biomechanical configuration . . . . .	233
3	Model I4: equivalent (von Mises) stress recorded for anterior right and left implants in complete muscle load set biomechanical configuration . . . . .	234
4	Model I4: equivalent (von Mises) stress recorded for posterior right and left implants in complete muscle load set biomechanical configuration . . . . .	235
5	Model I4: equivalent (von Mises) stress recorded for cancellous bone interface with posterior right and left implants in complete muscle load set biomechanical configuration . . . . .	236
6	Model I4c1: equivalent (von Mises) stress recorded for anterior right and left implants in complete muscle load set biomechanical configuration . . . . .	237
7	Model I4c1: micro-motions of posterior right and left axial implants in complete muscle load set biomechanical configuration . . . . .	238
8	Model I4c1: equivalent (von Mises) stress recorded for posterior right and left axial implants in complete muscle load set biomechanical configuration	239

---

9	Model I4c1: equivalent stress recorded for cancellous bone interface with posterior right and left implants in complete muscle load set biomechanical configuration . . . . .	240
10	Model I4: stress patterns on the surface of the posterior right angled implant at different time steps during clenching . . . . .	241
11	Model I4: equivalent stress along the implant socket of the posterior left implant . . . . .	242
12	Model I4: equivalent stress along the implant socket of the posterior right implant . . . . .	243
13	Model I4c1: equivalent stress along the implant socket of the posterior axial left implant . . . . .	244
14	Model I4c1: equivalent (von Mises) stress along the implant socket of the posterior axial right implant . . . . .	245
15	Model I4c1: equivalent stress relative to the cortical bone probed from the posterior axial right and left implant in complete muscle load set biomechanical configuration . . . . .	246
16	Model I4c2: equivalent stress along the implant socket of the longer posterior axial left implant . . . . .	247
17	Model I4c2: equivalent stress along the implant socket of the longer posterior axial right implant . . . . .	248
18	Model I1: equivalent stress along the implant socket of a deep cortical left implant . . . . .	249
19	Model I1: equivalent stress along the implant socket of a deep cortical right implant . . . . .	250
20	Model I1c1: equivalent stress along the implant socket of a mono- cortical left implant . . . . .	251
21	Model I1c1: equivalent stress along the implant socket of a mono-cortical right implant . . . . .	252

---

22	Model I1: equivalent stress generated on the right and left deep cortical implant during clenching. . . . .	253
23	Model I1: micro-motion generated on the left and right deep cortical implant during clenching. . . . .	254
24	Model I1: equivalent stress generated on the cancellous bone interface of the right and left deep cortical implant during clenching. . . . .	255
25	Model I1c1: equivalent stress generated on the left and right mono-cortical implant during clenching. . . . .	256
26	Model I1c1: micro-motion generated on the right and left mono-cortical implant during clenching. . . . .	257
27	Model I1c1: equivalent stress generated on the cancellous bone interface of the right and left mono-cortical implant during clenching. . . . .	258
28	General workflow for the computer-assisted surgery method (Part I) . . .	260
29	General workflow for the computer-assisted surgery method (Part II) . . .	261
30	Surgical navigation workflow including software/hardware interaction . .	262
31	Software workflow associated to the surgical navigation operation . . . .	263

# List of tables

2.1	Elastic moduli found by different studies for human femoral cortical bone.	27
2.2	Mechanical properties measured for femoral cortical bone by different studies. . . . .	28
2.3	Relation between age of the subject and mechanical properties of the cortical bone. . . . .	28
2.4	Range of femoral cancellous bone mechanical properties found by Cody (1996) . . . . .	29
2.5	Reference system used for the FEM. . . . .	34
2.6	Relationship between CT numbers and density for cancellous bone from different anatomical locations . . . . .	37
2.7	Modulus-density relationships according to several studies published in literature (from Helgason et al. 2008). . . . .	38
2.8	Experimental relationships between elastic modulus and strain rates. . . .	39
3.1	Material properties used in the mandibular FEA model for the bone tissues	53
3.2	Force vectors magnitudes during clenching . . . . .	54
3.3	Force vectors magnitudes during wide opening . . . . .	55
3.4	Force vectors used in simulating soft clenching action during scan . . . .	57
3.5	Muscle Force components used in simulating wide opening action during surgery . . . . .	58
3.6	Boundary conditions for the FEA modelling. . . . .	58
3.7	Maximum Von Mises stresses recorded during functional movements in Choi (2005). . . . .	65

---

3.8	Results for maximum distortion in the first and second molar region measured by FEA or with a number of different methods during clenching and wide opening movement compared with previous investigations. . . . .	67
3.9	Results for maximum von Mises stress in the first and second molar region during clenching and wide opening movement. . . . .	71
3.10	Results for maximum von Mises stress on the implant surface during clenching and wide opening movement. . . . .	71
3.11	Results for maximum equivalent stresses in case of a vertical hit . . . . .	74
3.12	Results for mandibular deformation in M3 during wide opening compared with the values obtained in M1. . . . .	82
3.13	Results for mandibular deformation for M3 during clenching compared with the valued obtained by M1. . . . .	82
3.14	Comparison of the stress values obtained for cortical and cancellous bone	88
4.1	Clenching model loads set . . . . .	124
4.2	Material properties used for the mandibular FEA model . . . . .	125
4.3	Deformation and stresses on implant surface and socket region in scenario I4	129
4.4	Deformation and stresses on implant surface and socket region in scenario I4c1 . . . . .	129
4.5	Results on implant surface and socket region in I4 using a simplified biomechanical configuration. . . . .	131
4.6	Results on implant surface and socket region in I4c1 using a simplified biomechanical configuration . . . . .	131
4.7	Fracture toughness, compression strength and elastic modulus maximum values found in literature for trabecular and cortical bone. . . . .	132
4.8	Deformation and stresses on implant surface and socket region in I4c2 . .	132
4.9	Deformation and stresses in I4c2 using a simplified biomechanical scenario	133
4.10	Deformation and stresses on implant surface and socket region in I1 using a complete clenching loads set . . . . .	133

---

4.11	Deformation and stresses on implant surface and socket region in I1c using a complete clenching loads set . . . . .	135
4.12	Deformation and stresses on implant surface and socket region in I1 using a simplified biomechanical configuration . . . . .	135
4.13	Deformation and stresses on implant surface and socket region in I1c using a simplified biomechanical configuration . . . . .	136
5.1	Comparison of the accuracies in mm for different systems for IGS and CAS found by Somogyi-Ganss (2015) . . . . .	152
5.2	Comparison of the accuracies in mm for different systems for IGS and CAS found by Ruppin (2008) . . . . .	153
5.3	<i>Source</i> of inaccuracies from CAS and IGS systems . . . . .	166
6.1	Calculation of surface points of three Titanium screws . . . . .	188
7.1	Results of the comparison between planned and placed implant position .	221
7.2	Extracted data on accuracy of two different image-guided surgery systems for oral implantology . . . . .	221